Central European Journal of Energetic Materials
ISSN 1733-7178; e-ISSN 2353-1843

Cent. Eur. J. Energ. Mater. 2022, *19*(2): 135-157; DOI 10.22211/cejem/150488
Article is available in PDF-format, in colour, at:
https://ipo.lukasiewicz.gov.pl/wydawnictwa/cejem-woluminy/vol-19-nr-2/

Research paper

A Study of a Protective Container for Combined Blast, Fragmentation and Thermal Effects from Energetic Materials Detonation

Khurshid Ahmed*), **Abdul Qadeer Malik**

National University of Sciences and Technology, Islamabad, PC 44000, Pakistan
** E-mail:* khurshid.phdscme@student.nust.edu.pk

ORCID information:
Ahmed K.: https://orcid.org/0000-0002-9604-7692

Abstract: A composite protective container is experimentally investigated to counter combined blast, fragmentation and thermal effects from either a 1.0 kg bare or 0.6 kg cased (pipe-bomb) TNT equivalent charge. Commercially available shaving foam was used as the internal filling material. The shaving foam quenched the initial fireball and afterburning reactions. The composite case contained the blast overpressure and prevented the escape of primary fragments. The novel combination of extended polystyrene (EPS) foam, bakelite and polyurethane (PU)-silica composite employed at the container base provided protection against in-contact explosive detonation. Maximum peak reflected overpressure of 86.87 kPa (12.6 psi) was measured at 1.0 m distance for 1.0 kg TNT equivalent charge detonation inside the container. The protective container provided 97% peak overpressure reduction compared to the equivalent surface burst detonation. The fragmentation and their impact on container were simulated using a coupled SPH-ALE approach. Steel casing fragments weighing up to 8.0 g with velocities in the range of 1260-1550 m/s were produced and impacted the container. This investigation provides a basis in the design of a device to combat terrorist devices in public places, high profile meeting venues and transportation systems.

Keywords: energetic materials, fireball, blast, fragmentation, container, mitigation

1 Introduction

The detonation of an energetic material, including improvised explosives devices (IEDs), results in formation of a fireball and the production of a blast wave. High velocity fragments are also produced if the energetic material is cased. Both these effects cause severe damage as surrounding objects are thrown violently, crushed or fragmented, leading to casualties-and structural damage [1]. Human beings are sensitive to overpressure as their air filled organs with the ears, lungs and gastrointestinal tract are the most susceptible to damage [2]. Thermal effects from the burning due to radiative heat and fireball, is another injury mechanism [3, 4] along with rapid propagating secondary fire. Fragmentation is the most lethal at-distance effect as energised fragments can travel significant distances and cause serious injury. In recent years, nails, screws, ball bearings and other objects have been used in IEDs to enhance fragment injury.

Overall, the quenching of the fireball along with blast wave mitigation at the detonation source is the most important manner to defeat these processes. A number of investigators have studied different classes of materials and threats in this area. Gelfand *et al.* [5] studied the blast wave mitigation properties of aqueous foam as a function of liquid fraction. Silnikov *et al.* [6, 7] and Takayama *et al.* [8] found multiphase material relaxation for blast mitigation in combined inhibitors to be effective. Ramadhan *et al.* [9] investigated the response of Kevlar/epoxy resin and aluminum alloy laminated panels at impact velocities up to 400 m/s. Alogla *et al.* [10] studied metallic protective panels against close blast loading, however, the effects of fragmentation was not addressed in this study. Elshenawy *et al.* [11] proposed a composite layer protection shelter against blast and fragments effects of a mortar warhead. Sun *et al.* [12] investigated the effectiveness of sandwich panels comprising aluminum alloy, steel and carbon fiber reinforced plastics (CFRP) against blast loading. Bornstein *et al.* [13] studied water-filled container against near-field blast loading. Langdon *et al.* [14] investigated numerically and experimentally the mitigation of damage in aircraft luggage containers subjected to internal blast loading. It was found that venting in containers along the aircraft body is more beneficial than lateral venting [14]. Qi *et al.* [15] investigated mitigation of shock loads from near field and contact detonations of high explosives using auxetic honeycomb-cored sandwich panels.

This combined shield was effective to protect reinforced concrete structures against impact and near field blast loadings [15]. Aqueous foam has been found effective to attenuate the blast wave [16-19].

The aqueous foam developed at Sandia National Labs in 1983 [20, 21] may not be available to general public or to first responders. Therefore, a commercially available health care product, Denim shaving foam, was considered in this study as blast mitigating medium. The blast mitigation capabilities of this foam has already been presented [4]. This present work deals with the numerical and experimental investigation of the blast, fragmentation and thermal effects mitigation with a container employing lightweight composite materials. The blast wave parameters of ~1.0 kg TNT equivalent surface burst were computed using CONWEP (Hyde [22]). ANSYS AUTODYN was used to numerically simulate the fragmentation of the steel cased charge (pipe-bomb) and its effects on the container. This is also an extension of the authors previous research on a scaled down model (Ahmed and Malik [23]).

2 Materials and Test Methods

The energetic materials studied were C4 and Comp-B. C4 ($C_{3.86}H_{7.57}N_{5.22}O_{5.32}$) is RDX based explosive. A cylindrical geometry was used in the present work with the density, velocity of detonation and Chapman-Jouget pressure being 1.46 g/cm^3, 7300 m/s and 19.98 GPa, respectively. Comp-B is a melt cast combination of RDX/TNT (60/40) with a density of 1.63 g/cm^3, detonation velocity and C-J pressure of 7570 m/s and 26.5 GPa, respectively.

The protective container comprised an inner and an outer cylinders. The inner layer was made of 3 mm thick mild steel (MS) with an inner diameter (ID) 500 mm and height of 350 mm. A 5 mm thick MS disc was welded at the bottom of the cylinder. Three steel tubes configuration 40 mm diameter and height, 120^o apart, were welded the bottom plate. Four layers of Kevlar woven fabric 470 GSM were wrapped around the exterior of the MS cylinder. The weight of the inner cylinder, shown in Figure 1, was 24.4 kg.

(a) (b)

Figure 1. MS cylinder (a) and inner container **(b)**

EPS foam 50 mm thick and of diameter ~490 mm was positioned on the bottom plate. Bakelite sheets measuring 380×295×20 mm and weighing 3.2 kg was then placed on EPS foam. Finally, a PU-silica disc prepared with 6 alternate layers of PU and silica was placed on the bakelite sheet. The measured density and compressive strength of PU-silica disc were 1.10 g/cm^3 and 232 MPa, respectively. The PU-silica sheet as shown in Figure 2(a) has shown good ductile behavior and toughness under compressive testing. Another EPS foam layer with thickness of 50 mm and diameter of 200 mm was then placed on the PU-silica composite. The EPS foam and bakelite sheets are shown in Figure 2(b).

(a) (b)

Figure 2. PU-silica disc (a) and EPS foam and bakelite sheet (b)

The proposed combination of composite materials, Kevlar fabric and laminated glass fiber reinforced polymer (GFRP), employed in this container were previously tested under extreme environment of blast and fragmentation produced by a scaled down artillery shell filled with 104 g of Comp-B explosive. The configuration, shown in Figure 3, was comprised 12 layers of Kevlar woven fabric wrapped on 5 mm thick GFRP and 6 mm thick PU foam. It was tested against the detonation of scaled down shell and has shown significant resistance to close-field blast loading and high velocity fragments penetration (Ahmed *et al.* [24]). A total of 26 fragments impacted the configuration and with only 8 being able to perforate. This layered combination of GFRP and Kevlar fabric was used in the container.

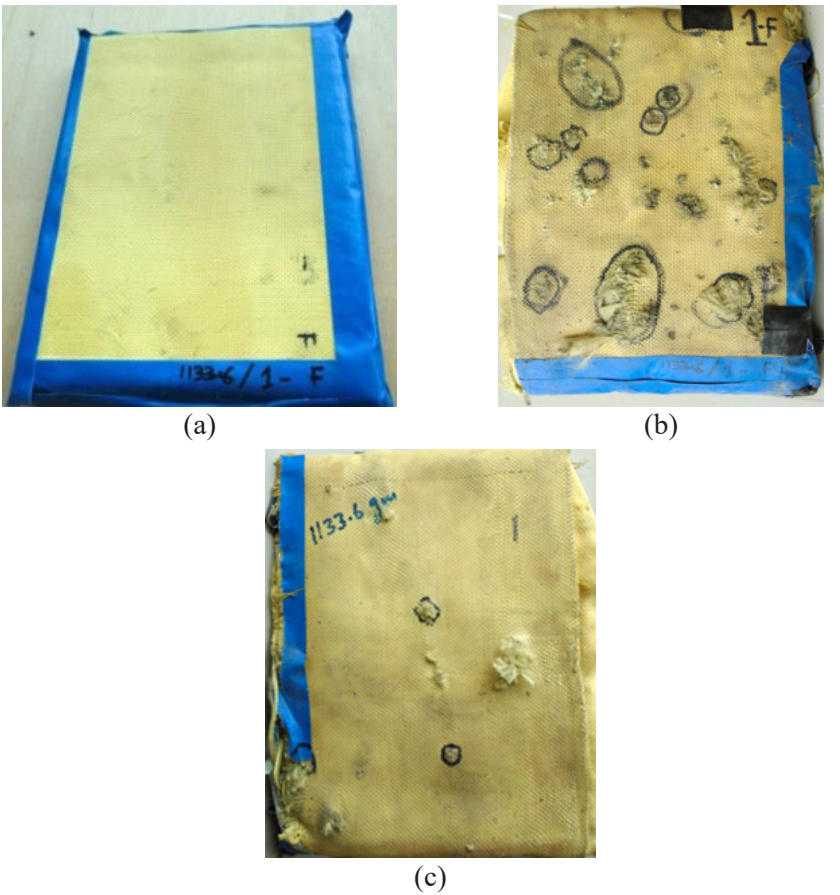

(a) (b)

(c)

Figure 3. Composite configuration tested against blast and fragments impact: before test (a) and front and back sides after fragments impact and penetration (b, c)

The outer cylinder was made of 8 mm thick laminated GFRP sheets with inner diameter 550 mm and height 800 mm. A single layer of Kevlar fabric 110 GSM was employed at the inner surface of the GFRP cylinder with silicon sealant. Eight layers of Kevlar fabric 470 GSM were wrapped on the outer surface of the GFRP cylinder shown in Figure 4. The top and bottom of the outer cylinder were left open. The outer container shown in Figure 4 weighed 34 kg.

(a)

(b)

(c)

Figure 4. GFRP cylinder (a), inner view of composite container (b) and outer composite container (c)

The inner cylinder was then placed inside the outer composite cylinder. The net weight of the combined container was 67 kg. C4 charge weighing 800 g (~1.0 kg TNT equivalent) was placed at the center of the container as shown in Figure 5(a). Shaving foam was then filled around the charge and inside the inner container as shown in Figure 5(b).

(a)

(b)

Figure 5. C4 placed inside container (a) and shaving foam filled around C4 (b)

The testing setup is shown in Figure 6. Three pressure transducers were placed 0.9 m above ground level at radial distances of 0.8, 0.9 and 1.0 m from center of charge. The transducers were positioned to measure the reflected blast overpressures (P_r).

(a) (b)

Figure 6. Experimental setup for 800 g C4 detonation inside container

To study the protective capability of the container against combined blast, fragmentation and thermal effects, a steel cased charge (pipe-bomb) was considered. The device shown in Figure 7 also simulates the effects of a lighter IED. The details of the steel cased charge are given in Table 1.

Figure 7. Steel cased charge (pipe-bomb)

Table 1. Material and dimensions of pipe-bomb for blast and fragmentation study

Material	Weight [g]	Length [mm]	OD [mm]	ID [mm]
Steel casing	1275	173	61	50
Comp-B filling	565	170	50	–

3 Numerical Simulations for the Steel Cased Charge (Pipe-bomb)

Optimizing the blast wave parameters and fragmentation characteristics of the pipe bomb presented in Figure 7 were not a primary focus of this experimental study. However, numerical simulations were performed to estimate these parameters. ANSYS AUTODYN [25] was used to simulate the blast and fragmentation of this steel cased charge (pipe-bomb), Ahmed *et al.* [24]. Jones-Wilkins-Lee (JWL) equation of state (EOS) was used for expansion of Comp-B product gases (Lee *et al.* [26]). The JWL EOS is given in Equation 1.

$$P = A\left(1 - \frac{\omega}{R_1 V}\right)e^{-R_1 V} + B\left(1 - \frac{\omega}{R_2 V}\right)e^{-R_2 V} + \frac{\omega E}{V} \tag{1}$$

where P and E are pressure and internal energy of the detonation products; A, B, R_1, R_2, ω are parametric constants, which depend on the type of explosive (Lee *et al.* [26] and Kravets *et al.* [27]).

The Shock EOS – Mie-Grüneisen form (Meyers [28]) was used as the EOS model for steel liner. This EOS as shown in Equation 2 is widely used for materials under shock loading.

$$P = P_H + \Gamma\rho(E - E_H) \tag{2}$$

Johnson-Cook strength model [29, 30] was used to simulate the behavior of the steel (AISI-1006) shell under the high strain rate loading of explosive detonation. The relationship presented in Equation 3 reproduced the strain hardening, strain rate and thermal softening effects of the steel casing.

$$\sigma_y = \left[A + B\varepsilon_p^n\right]\left[1 + C\ ln\ \varepsilon_p^*\right]\left[1 - T_H^m\right] \tag{3}$$

where A, B, C, n and m are constants for each material and T_H is homologous temperature. The Johnson-Cook failure model (Johnson *et al.* [29, 31]) shown in Equation 4 was used along with the strength model for casing material (AISI-1006). The material properties of steel-1006 were used from ANSYS AUTODYN library [25, 32].

$$\varepsilon_f = \left[D_1 + D_2\, e^{D_3\sigma^*}\right]\left[1 + D_4\, ln|\varepsilon^*|\right]\left[1 + D_5 T_H\right] \tag{4}$$

The values of constants *D1* to *D5* for steel-1006 were used from van der Voort *et al.* [33]. Kevlar layers were modeled with macro-homogeneous model that considers the whole layers are homogenous in geometry with orthotropic mechanical properties. Material properties for Kevlar and GFRP were used from Bresciani *et al.* [34], Soydan *et al.* [35] and Ansari *et al.* [36], respectively. PU foam was modeled with P-α compaction model. The material parameters were retrieved from ANSYS AUTODYN library [25, 37]. EPS was modelled using the crushable foam material model with a linear EOS. The parameters for the EPS were taken from Karagiozova *et al.* [38]. It has a compressive strength of 114 kPa at 10% strain. The EPS has density of 0.024 g/cm^3, bulk modulus was 5.390 MPa and the shear modulus 7.379 MPa [23, 39, 40].

ANSYS AUTODYN has the capability to generate fragment analysis in HTML format. The analysis comprised number of fragments, mass, kinetic energy, momentum, length, origin, coordinates and velocity of each fragment. A coupled SPH-ALE approach was employed to simulate the fragmentation of pipe bomb and the interaction of fragments with the inner container [23, 24, 41]. The SPH simulations of the fragmentation within the MS cylinder are shown in Figures 8-10.

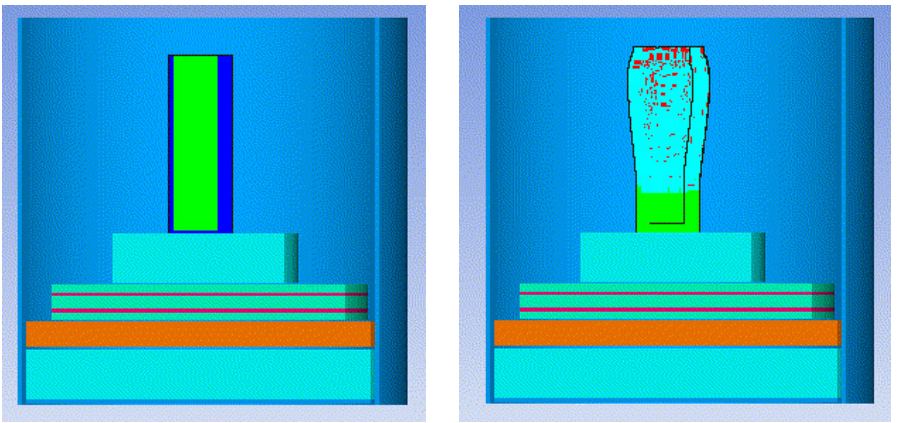

(a) (b)

Figure 8. SPH-ALE model for steel cased charge and inner container (a) and at 19 μs of detonation (b)

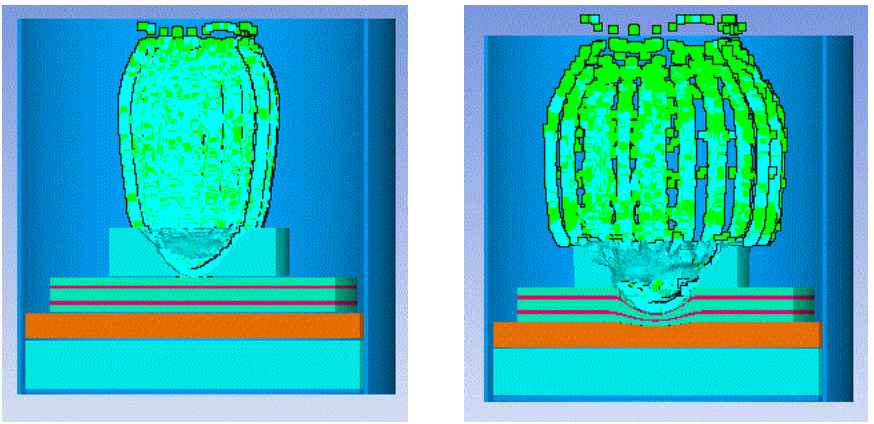

(a) (b)

Figure 9. Fragmentation at 58 μs (a) and expansion of fragments at 95 μs (b)

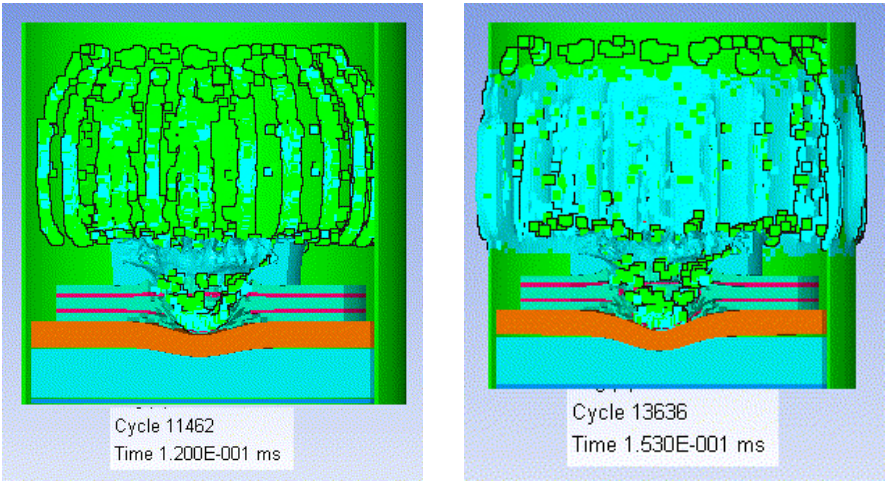

(a) (b)

Figure 10. Fragment expansion and impact on inner steel container

The fragmentation analysis in ANSYS AUTODYN has shown that a total of 732 fragments were produced with a distribution of mass ranging from few mg to 8.0 g. These fragments were grouped in four categories based on their weight:

– very small: <0.1 g,
– small: <0.1-1.0) g,
– medium <1.0-5.5> g,
– large: >5.5 g.

The number of fragments and their mass distribution is shown in Figure 11(a) while the velocity of the fragments is shown in Figure 11(b), most fragments had velocities of ~1550 m/s. The simulation results on fragment's mass and velocity distribution as well as the protective capabilities of the multi-layer configurations has been validated in references [23, 24, 42].

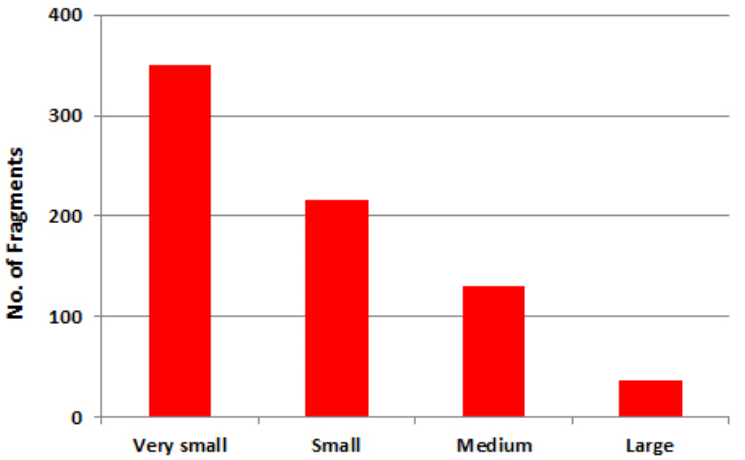

(a)

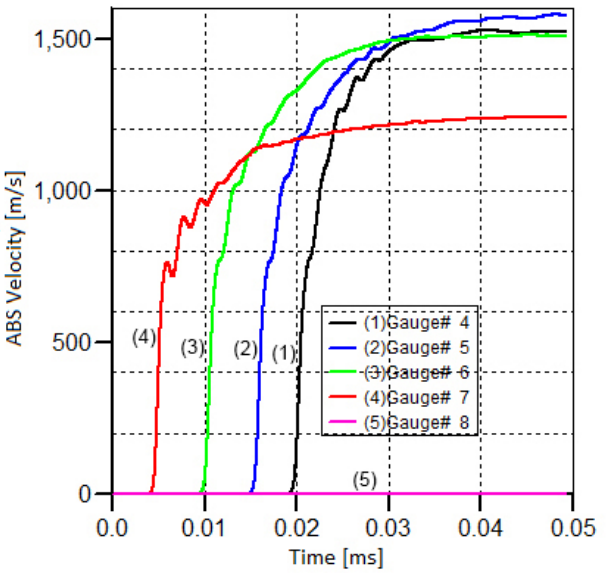

(b)

Figure 11. Fragments mass distribution (a) and fragments velocity plot (b)

4 Results and Discussion

Two experiments were performed with the container. In the first experiment, 800 g C4 (1.0 kg TNT equivalent) immersed in shaving foam was detonated inside the container. The shaving foam completely suppressed the fireball, and the container restricted the movement of product gases in lateral directions. C4 has an oxygen balance of −46.6%. The initial detonation products contain some unoxidised products; solid carbon (C), carbon monoxide (CO), hydrogen gas (H_2) *etc*. During the initial expansion these are further oxidized (*e.g.* C and CO to CO_2, H_2 to H_2O) through mixing with air thus producing additional heat. This process is called afterburning [4, 43]. The total heat of combustion is the sum of the detonation heat and afterburning heat. For C4 the heat of detonation is only 45% of the total combustion heat with the remaining 55% energy being produced by the afterburning reactions (Lebel *et al.* [43]).

The shaving foam completely suppressed the fireball and reduced the temperature owing to an energy transfer mechanisms inhibiting afterburning. The composite container restricted the movement of pressurized product gases in lateral directions. The gap between inner and outer cylinders allows the expansion of inner cylinder. This expansion under highly pressurized gases absorbs significant energy. The outer cylinder is therefore exposed to less severe loading. The high-speed images of the event at different time steps are shown in Figures 12(a-e).

The product gases emerge from the open top after 0.482 ms of C4 detonation. The expansion of carbonaceous soot with product gases is visible in the high-speed images, a further indication of the elimination of afterburning reactions. The outer layer of the Kevlar fabric was detached due to debonding probably *via* a spall-like mechanism. Figure 12(f) shows the post experiment view of the container.

There was a 40 mm gap between the base of the inner cylinder and ground level to allow expansion of MS base plate. However, the intense pressure detached the base plate from the cylinder. A minor leakage of the gases at the base was observed at late times. These gases were less pressurized and passed the 1.5 m radial distance after 35.0 ms from detonation.

The measured reflected overpressure and arrival time data is shown in Figure 13. A reflected overpressure peak of 175.8 kPa (25.5 psi) was recorded at 0.9 m from the charge center. A maximum reflected overpressure of 85.5 kPa (12.4 psi) was recorded at 1.0 m distance from the center of the container. As a comparison if the charge was detonated in open-air (without container) the peak reflected pressure at 1.0 m distance would be 4.86 MPa (705 psi) (Hyde [22]). The container has provided ≈97% reduction in overpressure.

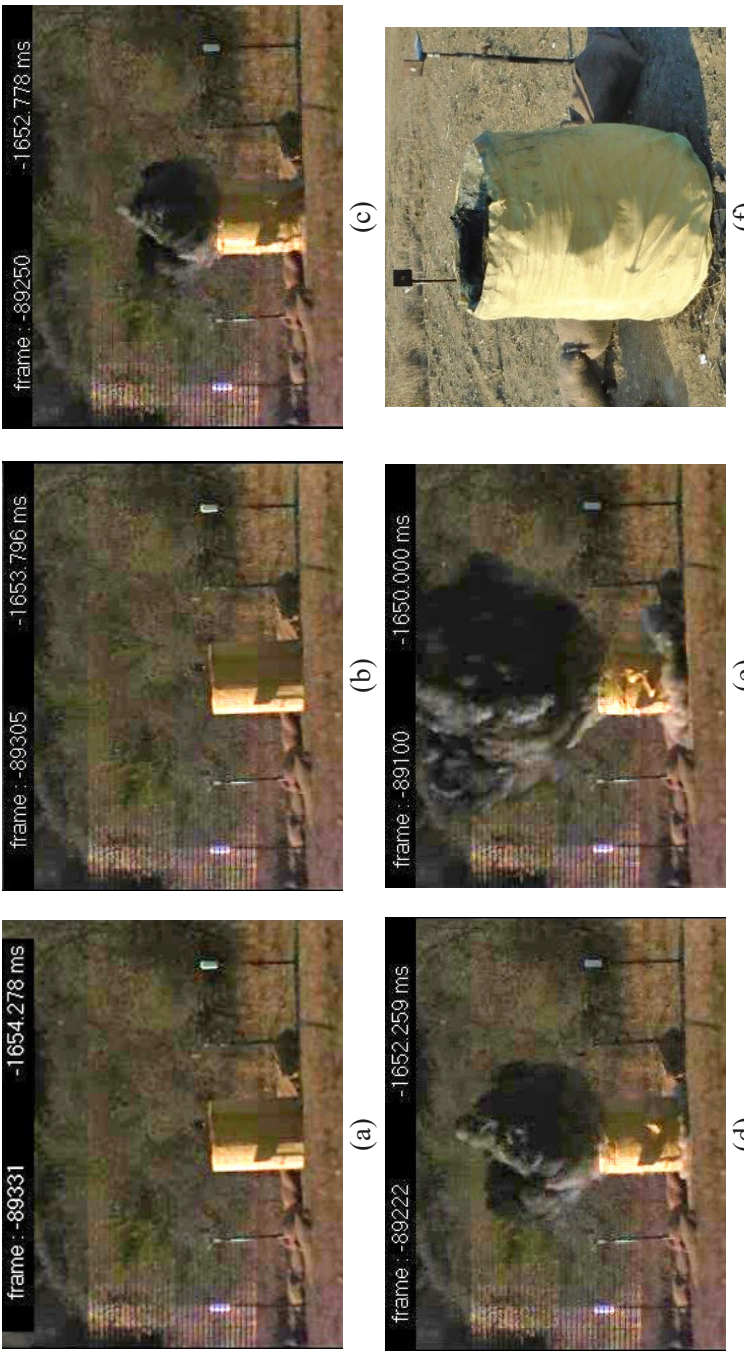

Figure 12. High-speed images of 800 g C4 detonation inside container at t equal: 0 (a), 0.482 (b), 1.50 (c), 2.0 (d), 4.2 ms (e) and still camera image of the container before test (f)

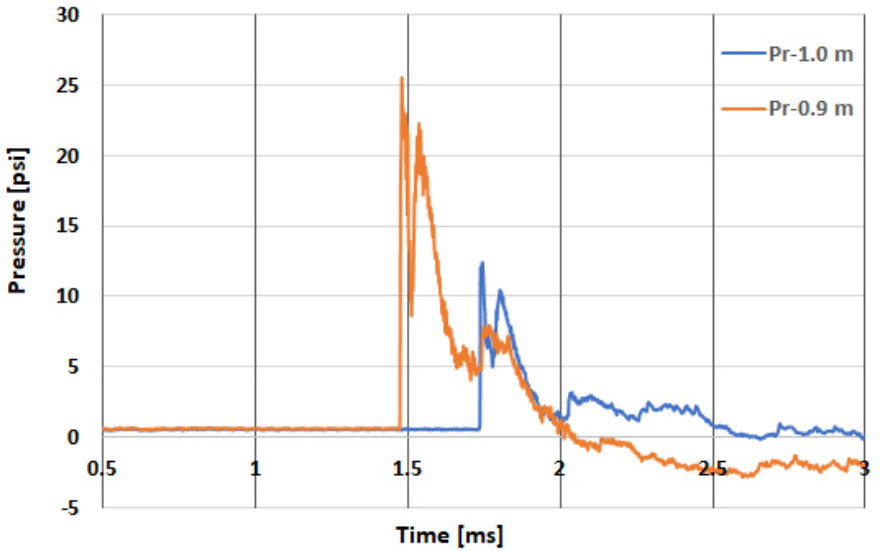

Figure 13. Reflected overpressure-time history for 800 g C4 detonation inside container

The second test was conducted by placing a steel cased charge (pipe bomb) inside the container. The overall strength of the container was already weakened by the explosive loading during the first experiment. An additional layer of GFRP was laid inside the MS cylinder for second test. The container filled with shaving foam and the testing setup is shown in Figure 14.

(a) (b)

Figure 14. Shaving foam filled around steel cased charge (a) and experimental setup (b)

Figure 15. High-speed images of steel cased 565 g Comp-B detonation inside container, at *t* equal: 0 (a), 0.407 (b), 0.648 (c), 1.222 (d), 2.500 (e) and 6.055 ms (f)

The amount of shaving foam filled for this test was relatively less as shown in Figure 14(a). That is why the fire ball was partially suppressed as can be seen from the high-speed images in Figure 15. However, the container still provided significant protection against overpressure. The appearance of a partially quenched fireball and the product gases containing carbonaceous soot from the open top are evident in Figures 15(b-e).

Although, the container collapsed during this test, there was no evidence of any debris flight beyond 1.5 m from the blast. The additional layer of GFRP inside the MS cylinder was able to offer considerable resistance against high velocity fragments. The outer composite container was able to contain most of the fragments. Only 13 fragments out of 732 were able to perforate the outer layer of Kevlar fabric as shown in Figure 16.

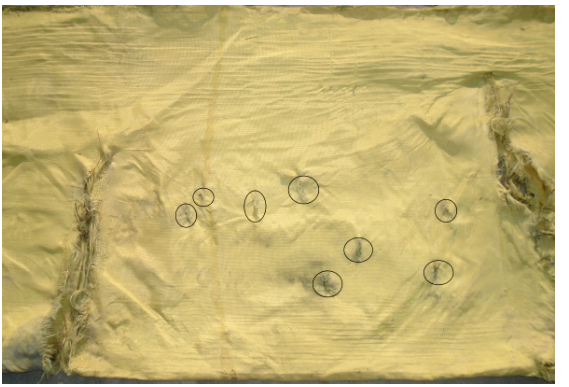

(a)

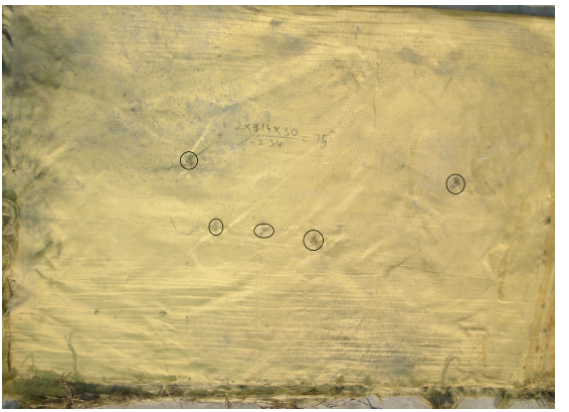

(b)

Figure 16. Fragments perforation through outer layer of Kevlar fabric

The container base was the most vulnerable place due to in contact detonation of C4. The combination of EPS foam, bakelite and PU-silica composite layers provided protection against the extreme loading conditions of C4 detonation. Although the MS disc at the bottom of the container was deformed, no signs of a fragment penetration were observed, as visible in Figure 17.

Figure 17. Bottom MS disc after second test

The maximum reflected overpressure measured at 0.85 m was 46.88 kPa (6.8 psi) at an arrival time of 1.21 ms. The first peak value at 0.9 m distance was 40 kPa (5.8 psi) with arrival time of 1.41 ms. The multiple reflections from the ground and the walls of the container yielded a reflected overpressure of 81.2 kPa (11.79 psi) at the distance of 0.9 m. The reflected overpressure-time history is shown in Figure 18.

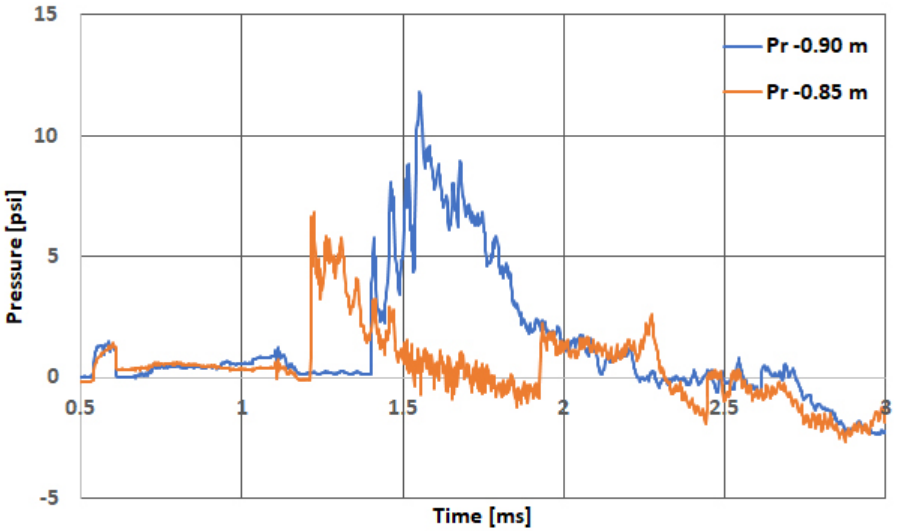

Figure 18. Reflected overpressure -time history for steel cased 565 g Comp-B charge inside container

Table 2 presents comparison of the present studies with CONWEP (Hyde [22]) results. A hemi-spherical surface burst was considered for CONWEP calculations. As the charge was positioned 166 mm above the ground level, the slant heights for CONWEP calculations corresponding to given radial distances of 1.0 and 0.9 m were 1.2 and 1.1 m, respectively. The transducers were 0.9 m above the ground level. Only reflected overpressures were measured experimentally.

Table 2. Comparison of experimental results with CONWEP calculations

W [kg TNT eq.]	CONWEP results – Surface Burst				with container		Reduction [%]
	R [m]	Ta [ms]	Ps [kPa]/[psi]	Pr [kPa]/[psi]	Ta [ms]	Pr [kPa]/[psi]	
1.0	1.0	0.65	917/133	4807/705	1.73	88.2/12.8	97
	0.9	0.55	1124/163	6481/940	1.48	176/25.5	98
0.6 (steel cased)	0.9	0.64	751/109	3930/570	1.41	81.3/11.79	97

As seen from the observed results the container was able to limit the devastating blast, fragmentation and thermal effects of 1.0 kg TNT equivalent of an energetic material detonation. In addition to bare charges,

the container also provided protection against fragment from cased charges of up to 0.6 kg TNT equivalent, pipe bomb and equivalent, low mass IEDs. The protective container provided 97% peak overpressure reduction compared to an equivalent surface burst detonation. The measured overpressures at 1.0 m distance were below the damage threshold. The research work provides ample data for the development of a blast mitigation system to combat terrorism against lighter time bomb/IEDs placed at public places, high profile meeting venues and transportation systems (land, air *etc*.).

5 Conclusions

- Two layers protective container was investigated experimentally and numerically to limit the combined blast, fragmentation and thermal effects of 1.0 kg bare or 0.6 kg steel cased TNT equivalent charge (pipe bomb) detonation. Commercially available shaving foam used as filling material in container has suppressed the fireball and eliminated the afterburning reactions. The laminated GFRP and Kevlar woven fabric presented significant strength against the escape of highly pressurized gases, blast wave and fragments in lateral directions.
- The protective container provided 97% peak overpressure reduction compared to an equivalent surface burst detonation. The C4 surface burst parameters were determined using CONWEP. The novel combination of EPS foam, bakelite and PU-silica layers provided protection against in contact C4 detonation at the container base.
- The pipe bomb fragmentation and impact on container was simulated in ANSYS AUTODYN using coupled SPH-ALE approach.
- The investigation would provide economical and lightweight protective mechanism towards safety of invaluable lives and critical structures against an energetic material detonation threats up to 1.0 kg TNT equivalent charge including time bomb/IEDs.

Acknowledgment

The authors are grateful and acknowledge the support of Mr. Mursaleen, Dr. Kamran, Dr. Javaid, Dr. Iram Raza Ahmad, Mr. Ashraf, Nusrat Iqbal and Kamran during the experimental work. The assistance of Ms Javeria is acknowledged and appreciated.

Declaration of competing interest

The authors declare that they have no known competing financial interests or personal relationships that could have appeared to influence the work reported in this paper.

References

[1] Zipf, R.K.; Cashdollar, K.L. *Effects of Blast Pressure on Structures and the Human Body.* [retrieved at http://citeseerx.ist.psu.edu/viewdoc/summary?doi=10.1.1.691.7547].

[2] Rutter, B. *Pressure versus Impulse Graph for Blast-induced Traumatic Brain Injury and Correlation to Observable Blast Injuries.* Doctoral Dissertation, Missuori University of Science and Technology, US, **2019**.

[3] Peters, P. Primary Blast Injury: An Intact Tympanic Membrane Does Not Indicate the Lack of a Pulmonary Blast Injury. *Mil. Med.* **2011**, *176*(1): 110-114.

[4] Ahmed, K.; Malik, A.Q. Experimental Studies on Blast Mitigation Capabilities of Conventional Dry Aqueous Foam. *AIP Adv.* **2020**, *10*(6), paper 065130: 1-19.

[5] Gelfand, B.; Silnikov, M.; Chernyshov, M. On the Efficiency of Semi-closed Blast Inhibitors. *Shock Waves* **2010**, *20*(4): 317-321.

[6] Silnikov, M.; Mikhailin, A.; Vasiliev, N.; Ermolaev, V.; Shishkin, V. Liquid Blast Inhibitors: Technology and Application. In: *Detection and Disposal of Improvised Explosives.* (Schubert, H.; Kuznetsov, A., Eds.) NATO Secur. Sci., Vol. 6, Springer, Dordrecht, **2006**, pp. 97-103.

[7] Silnikov, M.; Sadyrin, A.; Mikhaylin, A.; Orlov, A. Shock Wave Overpressure Evaluation at Blast Detonation Inside a Destructible Container. *Mater. Phys. Mech.* **2014**, *20*(2): 175-185.

[8] Takayama, K.; Silnikov, M.; Chernyshov, M. Experimental Study of Blast Mitigating Devices Based on Combined Construction. *Acta Astronaut.* **2016**, *126*: 541-545.

[9] Ramadhan, A.; Talib, A.A.; Rafie, A.M.; Zahari, R. High Velocity Impact Response of Kevlar-29/Epoxy and 6061-T6 Aluminum Laminated Panels. *Mater. Des.* **2013**, *43*: 307-321.

[10] Alogla, A.; Helal, M.; ElShafey, M.M.; Fathallah, E. Numerical Analysis for Critical Structures Protection against Blast Loading Using Metallic Panels. *Appl. Sci.* **2020**, *10*(6), paper 2121: 1-18.

[11] Elshenawy, T.; Abdo, G.; Aboelseoud, M. Ballistic Protection of Military Shelters from Mortar Fragmentation and Blast Effects using a Multi-layer Structure. *Def. Sci. J.* **2019**, *69*: 531-626.

[12] Sun, G.; Wang, E.; Zhang, J.; Li, S.; Zhang, Y.; Li, Q. Experimental Study on the Dynamic Responses of Foam Sandwich Panels with Different Facesheets and Core Gradients Subjected to Blast Impulse. *Int. J. Impact Eng.* **2020**, *135*, paper 103327: 1-20.

[13] Bornstein, H.; Di Placido, S.; Ryan, S.; Orifici, A.C.; Mouritz, A.P. Effect of Standoff on Near-Field Blast Mitigation Provided by Water-Filled Containers. *J. Appl. Mech.* **2019**, *86*(7), paper 071003: 1-10.
[14] Langdon, G.S.; Kriek, S.; Nurick, G.N. Influence of Venting on the Response of Scaled Aircraft Luggage Containers Subjected to Internal Blast Loading. *Int. J. Impact Eng.* **2020**, *141*, paper 103567: 1-15.
[15] Qi, C.; Remennikov, A.; Pei, L.-Z.; Yang, S.; Yu, Z.-H.; Ngo, T.D. Impact and Close-in Blast Response of Auxetic Honeycomb-cored Sandwich Panels: Experimental Tests and Numerical Simulations. *Compos. Struct.* **2017**, *180*: 161-178.
[16] Liverts, M. *Shock Wave Interaction with Aqueous Particulate Foams.* Ben-Gurion University of the Negev, **2012**.
[17] Liverts, M.; Ram, O.; Sadot, O.; Apazidis, N.; Ben-Dor, G. Mitigation of Exploding-Wire-generated Blast-waves by Aqueous Foam. *Phys. Fluids* **2015**, *27*(7): 076103.
[18] Sembian, S.; Liverts, M.; Apazidis, N. Attenuation of Strong External Blast by Foam Barriers. *Phys. Fluids* **2016**, *28*(9): 096105.
[19] Del Prete, E.; Chinnayya, A.; Domergue, L.; Hadjadj, A.; Haas, J.-F. Blast Wave Mitigation by Dry Aqueous Foams. *Shock Waves* **2013**, *23*(1): 39-53.
[20] Panczak, T.D.; Krier, H.; Butler, P.B. Shock Propagation and Blast Attenuation through Aqueous Foams. *J. Hazard. Mater.* **1987**, *14*(3): 321-336.
[21] Hartman, W.F.; Larsen, M.E.; Boughton, B.A. *Blast Mitigation Capabilities of Aqueous Foam.* Sandia National Laboratories, Report SAND2006-0533, **2006**.
[22] Hyde, D. *CONWEP: Conventional Weapons Effects Program.* US Army Engineer Waterways Experiment Station, USA, **1991**.
[23] Ahmed, K.; Malik, A.Q. Experimental Investigations of the Response of a Portable Container to Blast, Fragmentation, and Thermal Effects of Energetic Materials Detonation. *Int. J. Protective Struct.* **2022**, *13*(1): 45-64.
[24] Ahmed, K.; Malik, A.Q.; Hussain, A.; Ahmad, I.R.; Ahmad, I. Lightweight Protective Configurations Against Blast and Fragments Impact: Experimental and Numerical Studies. *AIP Adv.* **2020**, *10*(9): 095221.
[25] *Century Dynamics. Release 14.0 Documentation for ANSYS AUTODYN.* ANSYS Inc., US, **2011**.
[26] Lee, E.; Hornig, H.; Kury, J. *Adiabatic Expansion of High Explosive Detonation Products UCRL-50422*, University of California, California, **1968**.
[27] Kravets, V.; Zakusylo, R.; Sydorenko, Y.; Shukurov, A.; Sałaciński, T.; Zakusylo, D. Regularities of the Energy of Formation Field in the Explosion of a Conical Charge. *Cent. Eur. J. Energ. Mater.* **2019**, *16*(4): 533-546.
[28] Meyers, M.A. *Dynamic Behavior of Materials.* John Wiley & Sons, Inc., New York, Chichester, Brisbane, Toronto, Singapore, **1994**; ISBN 0-471-58262-X.
[29] Johnson, G.R.; Cook, W.H. A Constitutive Model and Data for Metals Subjected to Large Strains, High Strain Rates, and High Temperatures. *Proc. 7th Int. Symp. Ballistics*, Hague, **1983**.
[30] Murugesan, M.; Jung, D.W. Johnson Cook Material and Failure Model Parameters Estimation of AISI-1045 Medium Carbon Steel for Metal Forming Applications.

Materials **2019**, *12*(4): 609.
[31] Johnson, G.R.; Holmquist, T.J. An Improved Computational Constitutive Model for Brittle Materials. *AIP Conf. Proc., American Institute of Physics*, **1994**.
[32] Ahmed, K.; Malik, A.Q.; Ahmad, I.R. Heterogeneous Lightweight Configuration for Protection Against 7.62×39 mm Bullet Impact. *Int. J. Protective Structures* **2019**, *10*(3): 289-305.
[33] van der Voort, M.; Baker, E.; Collet, C. Fragmentation from Detonations and Less Violent Munition Responses (MSIAC Report 0-208). *IMEMTS*, Sevilla, Spain, **2019**.
[34] Bresciani, L.M.; Manes, A.; Ruggiero, A.; Iannitti, G.; Giglio, M. Experimental Tests and Numerical Modelling of Ballistic Impacts against Kevlar 29 Plain-woven Fabrics with an Epoxy Matrix: Macro-homogeneous and Meso-heterogeneous Approaches. *Composites, Part B* **2016**, *88*: 114-130.
[35] Soydan, A.M.; Tunaboylu, B.; Elsabagh, A.G.; Sarı, A.K.; Akdeniz, R. Simulation and Experimental Tests of Ballistic Impact on Composite Laminate Armor. *Adv. Mater. Sci. Eng.* **2018**, paper 4696143: 1-12.
[36] Ansari, M.M.; Chakrabarti, A.; Iqbal, M.A. Dynamic Response of Laminated GFRP Composite under Low Velocity Impact: Experimental and Numerical Study. *Procedia Eng.* **2017**, *173*: 153-160.
[37] Wai, B.C. *Investigation of Shock Wave Attenuation in Porous Media.* Naval Postgraduate College-NPS, **2009**.
[38] Karagiozova, D.; Nurick, G.; Langdon, G.; Yuen, S.C.K.; Chi, Y.; Bartle, S. Response of Flexible Sandwich-type Panels to Blast Loading. *Compos. Sci. Technol.* **2009**, *69*(6): 754-763.
[39] Bornstein, H.; Phillips, P.; Anderson, C. Evaluation of the Blast Mitigating Effects of Fluid Containers. *Int. J. Impact Eng.* **2015**, *75*: 222-228.
[40] Bornstein, H. *Physical Mechanisms for Near-field Blast Mitigation with Fluid-filled Containers.* RMIT University, Australia, **2018**.
[41] Becker, M.; Seidl, M.; Mehl, M.; Souli, M.h.; Legendre, J.-F. Numerical and Experimental Investigation of SPH, SPG, and FEM for High-velocity Impact Applications. *Proc. 12th European LS-DYNA Conf.*, **2019**.
[42] Ahmed, K.; Malik, Q.A.; Hussain, A.; Ahmad, I.R.; Ahmad, I. Blast and Fragmentation Studies of a Scaled Down Artillery Shell-Simulation and Experimental Approaches. *Int. J. Multiphys.* **2021**, *15*(1): 49-71.
[43] Lebel, L.S.; Brousseau, P.; Erhardt, L.; Andrews, W.S. Thermochemistry of the Combustion of Gas Phase and Condensed Phase Detonation Products in an Explosive Fireball. *Combust. Flame* **2014**, *161*(4): 1038-1047.

Received: March 23, 2021
Revised: May 27, 2022
First published online: June 28, 2022